CrossMark

Discovery of the Luminous, Decades-long, Extragalactic Radio Transient FIRST J141918.9+394036

C. J. Law[1,2] , B. M. Gaensler[2,3] , B. D. Metzger[4] , E. O. Ofek[5] , and L. Sironi[6]

[1] Department of Astronomy and Radio Astronomy Lab, University of California, Berkeley, CA 94720, USA
[2] Dunlap Institute for Astronomy and Astrophysics, University of Toronto, 50 St. George Street, Toronto, ON M5S 3H4, Canada; claw@astro.berkeley.edu
[3] Department of Astronomy and Astrophysics, University of Toronto, 50 St. George Street, Toronto, ON M5S 3H4, Canada
[4] Department of Physics and Columbia Astrophysics Laboratory, Columbia University, New York, NY 10027, USA
[5] Benoziyo Center for Astrophysics, Weizmann Institute of Science, 76100 Rehovot, Israel
[6] Department of Astronomy, Columbia University, New York, NY 10027, USA

Abstract

We present the discovery of a slowly evolving, extragalactic radio transient, FIRST J141918.9+394036, identified by comparing a catalog of radio sources in nearby galaxies against new observations from the Very Large Array Sky Survey. Analysis of other archival data shows that FIRST J141918.9+394036 faded by a factor of $\sim$50 over 23 years, from a flux of $\sim$26 mJy at 1.4 GHz in 1993 to an upper limit of 0.4 mJy at 3 GHz in 2017. FIRST J141918.9+394036 is likely associated with the small star-forming galaxy SDSS J141918.81+394035.8 at a redshift $z = 0.01957$ ($d = 87$ Mpc), which implies a peak luminosity $\nu L_\nu \gtrsim 3 \times 10^{38}$ erg s^{-1}. If interpreted as an isotropic synchrotron blast wave, the source requires an explosion of kinetic energy $\sim 10^{51}$ erg some time prior to our first detection in late 1993. This explosion is most likely associated with a long gamma-ray burst (GRB), but the radio source could also be interpreted as the nebula of a newly born magnetar. The radio discovery of either of these phenomena would be unprecedented. Joint consideration of the event light curve, host galaxy, lack of a counterpart GRB, and volumetric rate suggests that FIRST J141918.9+394036 is the afterglow of an off-axis ("orphan") long GRB. The long time baseline of this event offers the best available constraint in afterglow evolution as the bulk of shock-accelerated electrons become non-relativistic. The proximity, age, and precise localization of FIRST J141918.9+394036 make it a key object for understanding the aftermath of rare classes of stellar explosion.

Key words: catalogs – gamma-ray burst: general – radio continuum: general – stars: magnetars – surveys

1. Introduction

Multiple large radio interferometric surveys were conducted in the 1990s with sufficiently high spatial resolution to facilitate comparison to optical surveys. These first robust statistical samples enabled novel tests of the physics of high-redshift quasars (Becker et al. 2000), star-forming galaxies (Appleton et al. 2004), Galactic pulsars (Kaplan et al. 2000), constraints on the beaming factors of gamma-ray bursts (GRBs; Gal-Yam et al. 2006), and more. Today, a new generation of high-energy, optical, and radio sky surveys are being conducted with a focus on sensitivity to time-domain phenomena like supernovae and GRBs (Gehrels et al. 2004; Law et al. 2009; Mooley et al. 2016). The Karl G. Jansky Very Large Array (VLA) is in the midst of a sky survey (VLASS) whose design explicitly supports transient science (M. Lacy 2018, in preparation).

Transient surveys at optical and high energies have revolutionized our understanding of relativistic transients like GRBs (Woosley & Bloom 2006) and tidal disruption events (TDEs; van Velzen et al. 2011; Zauderer et al. 2011), but they are less sensitive to the vast majority of events not beamed in our direction (Frail et al. 2001). In contrast, radio emission traces the total kinetic energy (*calorimetry*) of the interaction of ejecta with the interstellar medium (ISM). This makes radio observations valuable for transient discovery and unbiased rate estimates (Frail et al. 2005). Even non-relativistic explosions, such as the hypothesized magnetar-powered supernovae (Kasen & Bildsten 2010), may produce radio emission at late times, once the supernova ejecta become transparent to free–free absorption and the birth nebula of the inner engine is revealed (Murase et al. 2016; Metzger et al. 2017; Nicholl et al. 2017a; Omand et al. 2018). The recent association of a fast radio burst (FRB; Chatterjee et al. 2017) with a luminous, persistent radio source has suggested that such slowly evolving radio transients may provide signposts for the discovery of past energetic events giving birth to FRB sources (Kashiyama & Murase 2017; Margalit et al. 2018).

Tremendous effort has been invested in blind radio transient surveys (Bower et al. 2010; Croft et al. 2010; Bell et al. 2011; Ofek et al. 2011; Mooley et al. 2013; Rowlinson et al. 2016; Murphy et al. 2017), but the requirements are severe. For example, orphan-GRB afterglows require a search at mJy-sensitivity, over 10^4 deg^2, with multiple epochs over many years (Levinson et al. 2002; Metzger et al. 2015b). This class of radio survey is only becoming available today by comparison of VLA surveys from the 1990s (Becker et al. 1995; Condon et al. 1998) to the VLASS.

Ofek (2017) collected a sample of galaxies with luminosity distance smaller than 108 Mpc ($z = 0.025$) and compared them to point sources in the VLA Faint Images of the Radio Sky at Twenty-Centimeters (FIRST) survey (Becker et al. 1995). He identified a set of radio sources with potential association to nearby galaxies and relatively high luminosities ($\nu L_\nu > 3 \times 10^{37}$ erg s^{-1}). Here, we describe the analysis of new data from

Table 1
VLASS Observations of Ofek (2017) Sources

Source Designation in FIRST	$S_{\text{FIRST}}^{\text{a}}$ (mJy)	$S_{\text{VLASS}}^{\text{b}}$ (mJy)	Spectral Index
J092758.2−022558	2.1	1.54	−0.4
J104726.6+060247	2.9	1.08	−1.3
J235351.4+075835	4.2	3.19	−0.4
J131441.9+295959	2.2	1.83	−0.2
J162244.5+321259.	2.0	1.23	−0.6
J141918.9+394036	20.11	<0.4	<−5.1

Notes.
[a] Typical FIRST peak flux density error is 0.14 mJy.
[b] Typical VLASS peak flux density error in quick-look images is 0.12 mJy (statistical) plus 10% (systematic).

VLASS and archival radio data that reveals that one of these sources, FIRST J141918.9+394036 (hereafter J1419+3940), is a luminous radio transient. Section 2 describes how we discovered the transient by its disappearance in VLASS, and Section 3 presents a radio light curve compiled from multiple telescopes with detections spanning more than two decades. We also describe the properties of the host galaxy of J1419+3940, constraints on gamma-ray and X-ray emission, and an estimate of the volumetric rate for J1419+3940-like transients. Section 4 presents calculations and modeling of the radio data that suggests that J1419+3940 is either the afterglow of an orphan GRB, or is the wind nebula produced in the aftermath of a magnetar-powered supernova. We summarize the results and present future tests of this model in Section 5. Computational (Jupyter) notebooks to reproduce the analysis presented here can be found at https://github.com/caseyjlaw/vlass_query.

2. Discovery

The first precise localization of an FRB revealed an unambiguous association with a luminous, persistent synchrotron radio source (Chatterjee et al. 2017). Under the assumption that at least a subset of FRBs should have luminous persistent radio counterparts, Ofek (2017) identified 122 potential FRB hosts by identifying radio sources seen toward galaxies. In most cases, the radio sources are active galactic nuclei that reside in the centers of their host galaxies. However, 11 of these sources were designated as potentially interesting as FRB counterparts because they were not located in their host's nucleus. Of those 11, J1419+3940 was identified as being the most similar to the one known persistent counterpart to an FRB, both in its luminosity and its association with a small, star-forming galaxy.

The VLA Sky Survey started observations in late 2017 and the first epoch (epoch 1.1) covers 50% of the observable sky over the frequency range 2 to 4 GHz to a 1σ sensitivity of 120 μJy beam^{-1}. Pipeline processed images are made available publicly within two weeks of observation. We searched these images for counterparts to the 11 most interesting sources in Ofek (2017). Six of the 11 sources have VLASS coverage in epoch 1.1 and are summarized in Table 1. All of the sources with VLASS coverage have a 3 GHz flux less than that of the 1.4 GHz flux measured in the FIRST survey. Assuming no variability between FIRST and VLASS, all but one source have implied spectral indexes ($\alpha_{1.4/3\,\text{GHz}}$ for $S_\nu \propto \nu^\alpha$) range from −0.2 to −1.3.

One of the sources in Table 1, FIRST J141918.9+394036, is not detected at 3 GHz to a nominal 3σ limit of 0.37 mJy. We measured fluxes in VLASS quick-look images with fluxes

Table 2
Radio Observations of J1419+3940

| Telescope	Date (year)	Freq. (GHz)	Peak Flux (mJy)	Observation Name
TI	1975	0.365	<400	Texas Survey
N. Cross	1977	0.408	<100	Bologna Sky Survey
NRAO 91m	1983.3	1.4	<100	Green Bank Northern Sky Survey (GBNSS)
NRAO 91m	1987	4.85	<25	Green Bank 6 cm Survey (GB6)
MSRT	1993.03	0.232	<180	Miyun Survey
VLA	1993.87	1.465	26 ± 2	AB6860
VLA	1993.87	0.325	<174	AB6860
WSRT	1994.31	0.325	<9	Westerbork Northern Sky Survey (WENSS)
VLA	1994.63	1.40	20.77 ± 0.17	FIRST Survey
VLA	1995.32	1.40	16.10 ± 0.51	National Radio Astronomy Observatory (NRAO) Very Large Array (VLA) Sky Survey (NVSS)
VLA	2005.20	0.074	<74	VLA Low-Frequency Sky Survey Redux (VLSSr)
WSRT	2008.54	1.415	2.5 ± 0.2	ATLAS-3D[a]
ATA	2009.12	1.43	<12	Allen Telescope Array Twenty-centimeter Survey (ATATS)
WSRT	2010.53	1.415	2.1 ± 0.2	ATLAS-3D
WSRT	2010.55	1.415	1.9 ± 0.2	ATLAS-3D
WSRT	2010.57	1.415	1.9 ± 0.2	ATLAS-3D
WSRT	2010.59	1.415	1.4 ± 0.2	ATLAS-3D
WSRT	2010.59	1.415	1.2 ± 0.2	ATLAS-3D
WSRT	2010.61	1.415	1.5 ± 0.2	ATLAS-3D
WSRT	2010.71	1.415	1.6 ± 0.2	ATLAS-3D
WSRT	2010.79	1.415	1.8 ± 0.2	ATLAS-3D
WSRT	2010.82	1.415	1.9 ± 0.2	ATLAS-3D
GMRT	2011.29	0.15	<30	Tata Institute of Fundamental Research (TIFT) Giant Metrewave Radio Telescope (GMRT) Sky Survey (TGSS)
VLA	2015.36	1.52	1.1 ± 0.1	15A-033
VLA	2015.36	3.0	0.75 ± 0.05	15A-033
VLA	2017.78	3.0	<0.4	VLASS, epoch 1.1

Note. All of the fluxes have been corrected for primary-beam attenuation. Upper limits are as quoted in the original work, or 3σ when derived from our own analysis.
[a] The quoted ATLAS-3D flux density errors include an estimate of systematic error added in quadrature to the typical statistical error of 0.1 mJy.

References. Texas Survey (Douglas et al. 1996), Bologna Sky Survey (Ficarra et al. 1985), GB6 (Becker et al. 1991; Gregory et al. 1996), GBNSS (Condon & Broderick 1985; White & Becker 1992), Miyun Survey (Zhang et al. 1997), FIRST (Becker et al. 1995), WENSS (Rengelink et al. 1997), NVSS (Condon et al. 1998), VLSSr (Lane et al. 2014), TGSS (Intema et al. 2017), VLASS (M. Lacy 2018, in preparation), ATLAS-3D (Serra et al. 2012), ATATS (Croft et al. 2010).

accurate to 10% (M. Lacy 2018, in preparation), so we estimate a 3 GHz upper limit of 0.4 mJy. The nondetection implies a factor of 50 drop relative to the FIRST survey,[7] equivalent to a

---

[7] Spurious variables and transients were found in FIRST data prior to 2012 (see Ofek et al. 2010), but those issues have now been corrected (Helfand et al. 2015).
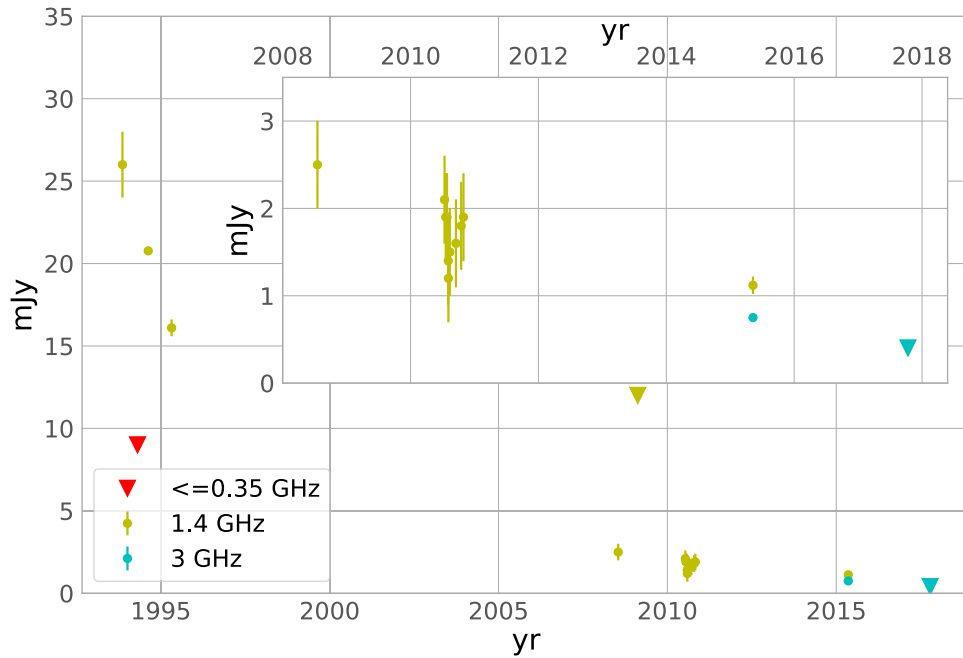
Figure 1. Flux density of J1419+3940 as a function of time, starting with our first detection in 1993. Observing frequencies are shown in three broad ranges ($\leqslant$350 MHz, 1.4 GHz, 3 GHz) encoded with different colors. Upper limits are shown as triangles and detections as circles. Not shown are five upper limits measured between 1977 and 1987 and three of the upper limits at low frequencies determined after 1993. The inset figure shows a closer view of the detections made over the last decade.

factor of 30 drop at fixed frequency (assuming a typical synchrotron spectral index of -0.7). The magnitude of this drop is highly anomalous, and motivated us to search other archival radio data to more fully characterize this source.

3. Characterization

3.1. Radio Transient

As shown in Table 2 and Figure 1, the position of J1419+3940 has been observed at 24 other epochs by eight different telescopes over more than four decades. This includes both wide-field sky surveys and serendipitous observations recovered from archives. Below, we describe the analysis of these radio observations.

3.1.1. VLA Surveys

In addition to the FIRST and VLASS sky surveys discussed above, J1419+3940 was observed and detected by the NRAO-VLA Sky Survey at 1.4 GHz (NVSS; Condon et al. 1998). We downloaded images from all three VLA surveys and used `Aegean` (Hancock et al. 2018) to fit a 2D Gaussian to the total intensity counterpart of J1419+3940 in NVSS, designated NVSS J141918 +394036 (see Table 2). We also examined the channel-averaged linear polarization data from NVSS, and see no signal in Stokes Q or U down to a 5-σ sensitivity of 1.5 mJy, corresponding to an upper limit on the linearly polarized fraction of 9%.

The most precise localization is measured by FIRST, which finds (R.A. J2000, decl. J2000) = (14:19:18.855, +39:40:36.0) with an uncertainty of $0\overset{''}{.}3$ (dominated by systematics at 1/20 of beam size; White et al. 1997). We queried the NRAO archive and found that repeated observations toward J1419+3940 *within* the FIRST and NVSS surveys fell within a one week span. A separate analysis of repeated FIRST observations did not reveal J1419 +3940 as variable on that timescale (Thyagarajan et al. 2011).

3.1.2. Other Sky Surveys

In the 1980s, the NRAO 91 m telescope was used to conduct sky surveys at 1.4 and 4.85 GHz (Condon & Broderick 1985; Becker et al. 1991). These surveys are interesting because they were relatively sensitive and observed only a few years before the first VLA detection of J1419+3940 in the 1990s. J1419 +3940 was not detected in these surveys to limiting flux densities of 100 and 25 mJy at 1.4 and 4.85 GHz, respectively.

Six other sky surveys observed the position of J1419+3940 at frequencies below 1 GHz: the VLA at 74 MHz (VLSSr), the GMRT at 150 MHz (TGSS), the MSRT at 232 MHz (Miyun Survey), WSRT at 325 MHz (WENSS), the Texas Interferometer at 365 MHz (Texas Survey), and the Northern Cross at 408 MHz (Bologna Sky Survey). None of these surveys detected the transient (see Table 2).

WENSS is not only the most sensitive of the low-frequency surveys, but it observed this field within a few months of VLA observations near the (apparent) peak brightness at 1.4 GHz. Assuming the J1419+3940 radio brightness changes slowly, the WSRT and FIRST observations are effectively simultaneous and the WSRT nondetection limits the spectral index near peak flux, $\alpha_{0.35/1.4} > +0.6$.

The Allen Telescope Array (ATA) observed J1419+3940 as part of a 690 deg^2 region at 1.4 GHz (the ATATS survey; Croft et al. 2010). No counterpart was detected above its 3σ flux density upper limit of 12 mJy.

3.1.3. WSRT Archives

A search of the WSRT archives revealed a series of observations of NGC 5582 (roughly $10'$ away) as part of the ATLAS-3D project (Serra et al. 2012). In total, 10 epochs of observing were made in 2008 and 2010 with a bandwidth of 20 MHz centered at 1.415 GHz (T. Oosterloo, R. Morganti and P. Serra, 2018, in preparation). The data, which are in total intensity only, were calibrated and corrected for primary-beam

attenuation with MIRIAD (Sault et al. 1995), and images at each epoch detect J1419+3940 with a significance of roughly 20σ.

We modeled the source in FITS images with Aegean and quote peak flux densities in Table 2. The statistical errors are roughly 0.1 mJy, but a joint analysis of all sources in the field suggests that there are significant systematic effects as well. We find that the standard deviation of peak flux for all sources scales with brightness and has a minimum of 0.2 mJy. We add this value to the statistical error in quadrature for all analysis presented here.

The WSRT fluxes for J1419+3940 in Table 2 do not show a purely secular decay, but instead suggest some small level of gradual variability up and down across epochs. To assess the possibility of short-term flux variability, we identified 22 other unresolved sources within the WSRT field of view, each detected at all or almost all epochs, and ranging in flux from 1 to 380 mJy. For each source, we extracted fluxes at each epoch, and computed the mean flux μ, standard deviation σ, and modulation index $m \equiv \sigma/\mu$. J1419+3940 has $m = 0.21$, which is larger than for any of the other 22 sources, for which the mean value is $m = 0.10 \pm 0.05$. However, the first flux measurement was made two years prior to the others, so the apparent long-term decay of the flux of J1419+3940 increases the modulation index. If we disregard the flux point from 1998, we find $m = 0.17$ for J1419+3940, which is comparable to that for other millijansky sources in the field: for example, FIRST J142131.9+392355 has a mean WSRT flux of 1.5 mJy with $m = 0.20$ and a randomly jittering flux across the WSRT epochs, but has a somewhat different FIRST flux of 2.3 mJy. On the other hand, FIRST J142103.2+392448 has $\mu = 2.2$ mJy and $m = 0.15$ with a smoothly varying light curve like seen for J1419+3940, but has a similar FIRST flux of 2.3 mJy. Overall, we conclude that there is the suggestive possibility from the data that J1419+3940 exhibits flux variability, but we cannot definitively confirm or rule out such behavior from the WSRT data.

3.1.4. VLA Archives

A search of the VLA archives revealed two VLA observing campaigns with useful data toward J1419+3940. The first of these is a legacy VLA observation AB6860, which was observed in 1993 November (about nine months earlier than FIRST), at both 325 MHz and 1.4 GHz.

We analyzed the AB6860 observations in MIRIAD and detected the source with a significance of 40σ at 1.4 GHz (the 325 MHz observations result only in an upper limit). The AB6860 observations did not contain a flux calibrator, so the flux scale is estimated via considering the fluxes of six field sources, all detected as unresolved objects in the FIRST, NVSS, and 10 WRST observations described above. Two of these sources (FIRST J141858.8+394626 and FIRST J142006.4+393503) show significant (>50%) changes in flux between epochs, and are assumed to be variable sources. The remaining four sources (FIRST J142009.3+392738, FIRST J142030.5+400333, FIRST J142120.6+394110, and FIRST J142123.5+393332) have consistent fluxes at 1.4 GHz across all 12 epochs of approximately 35, 12, 15 and 380 mJy, respectively. Setting the fluxes of these four sources to these values in the AB6860 data, we determine a 1.4 GHz flux for J1419+3940 at epoch 1993.87 of 27 mJy. We note though that there is a 4%–5% difference in observing frequency between
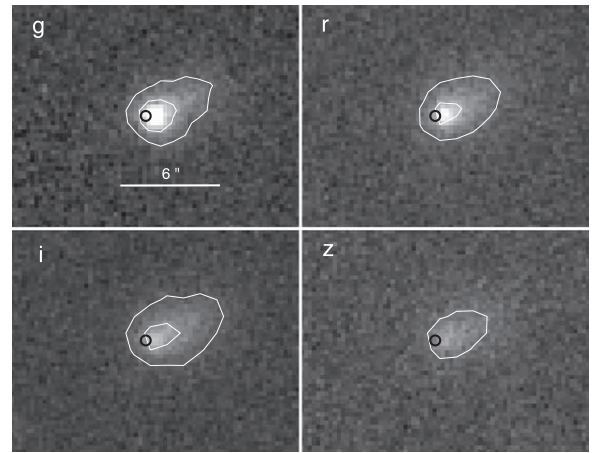
Figure 2. Comparison of J1419+3940 and its host galaxy as seen by Pan-STARRS in g, r, i, and z bands. Each panel is centered on the stacked position of SDSS J141918.81+394035.8 (a.k.a. PSO J141918.804+394035.996) with contours at 3 and 10 times the noise in each image. The FIRST radio localization of J1419+3940 is shown as a black circle with radius 0$\farcs$3.

the AB6860 observations and these other data (see Table 2). Assuming a typical radio galaxy spectral index for these four calibration sources of –0.7, and using the scatter between the flux measurements from FIRST, NVSS, and WSRT as an estimate of the uncertainties, we determine a 1.4 GHz flux for J1419+3940 at this epoch of 26 ± 2 mJy as listed in Table 2. We see no linearly or circularly polarized emission from J1419+3940 in these data above a 5σ limit of ~4 mJy, corresponding to a fractional upper limit of ~15%.

The second archival VLA observation was conducted at 1.4 and 3.0 GHz in 2015 (a "Jansky" VLA project designated 15A-033[8]). We calibrated and imaged this observation using CASA (McMullin et al. 2007). J1419+3940 is detected in both the 1.4 and 3 GHz bands at a brightness of about 1 mJy with a significance of 10–15σ. The mean flux across the 1.4 and 3 GHz bands implies a spectral index of $\alpha_{1.4/3} = -0.6 \pm 0.2$. This late-time spectral index measurement has changed significantly from the early lower limits on the spectral index between 0.35 and 1.4 GHz.

3.2. Association with a Host Galaxy

J1419+3940 is located 0$\farcs$5 from the center of the galaxy SDSS J141918.81+394035.8 (Abolfathi et al. 2018) with an r-band magnitude ~19. The galaxy is also detected by Pan-STARRS (Chambers et al. 2016), the Dark Energy Camera Legacy Survey (DECaLS; Dey et al. 2018), the intermediate Palomar Transient Factory (iPTF; Masci et al. 2017), and the USNO-B Survey (Monet et al. 2003). Figure 2 shows the association of J1419+3940 with the galaxy. The iPTF DR3 catalog shows it was detected in 34 epochs spanning 2.3 years around 2009 and had no significant variability. The USNO-B1 catalog shows that the galaxy had a similar magnitude in 1979.

A Sloan Digital Sky Survey (SDSS) spectrum of the galaxy[9] finds strong emission lines indicative of active star formation. These lines provide a robust redshift measurement of $z = 0.01957$ (a distance of 87 Mpc using $H_0 = 67.4 \, \mathrm{km \, s^{-1} \, Mpc^{-1}}$;

---

[8] In a remarkable coincidence, one of us (B.M.G.) was a co-investigator on this archival observation.
[9] See https://dr9.sdss.org/spectrumDetail?plateid=1380&mjd=53084&fiber=534.

Planck Collaboration et al. 2018). At this distance, the galaxy has an extinction-corrected absolute r-band magnitude of -16 and a size of about 2.5 kpc ($6''$ in projection). The g- and r-band optical images show a clear enhancement on the east side of the galaxy that is coincident with J1419+3940. Dwarf galaxies such as this one can host supermassive black holes (e.g., Henize 2–10; Reines et al. 2016), but an enhancement at the galaxy's edge is more likely to be an area of enhanced star formation.

SDSS J141918.81+394035.8 is also detected by *WISE*,[10] which allowed Chang et al. (2015) to combine with SDSS data to model this galaxy's star formation properties. They find that SDSS J141918.81+394035.8 has a stellar mass $\log M/M_\odot = 7.24 \pm 0.11$, a star formation rate (SFR) $\log \text{SFR}/(M_\odot \text{ yr}^{-1}) = -1.2^{+0.16}_{-0.2}$, and specific star formation rate $\log \text{sSFR}/\text{yr}^{-1} = -8.4 \pm 0.2$ (95% confidence intervals). The low mass and high specific SFR make this galaxy similar to the typical host galaxies of long GRBs and superluminous supernovae (Japelj et al. 2016). The location of J1419+3940 in its host, the host mass, and SFR are all similar to the association of FRB 121102 and its host galaxy (Bassa et al. 2017).

Within the $1.1 \times 10^4 \text{ deg}^2$ surveyed by FIRST, there are about 2.5×10^5 compact sources (deconvolved size less 3 times its error) brighter than 1.3 mJy (10σ). Ofek (2017) define a "nuclear association" as any radio source located within $1''$ of the galaxy centroid, a definition that includes J1419+3940. Given the density of compact FIRST sources, the number of chance nuclear associations with the Ofek (2017) spectroscopic catalog (28,815 galaxies) is roughly 0.16. The actual number of such associations is 85, so all them are likely physically associated. Although variability was not a selection criterion, we note that variable FIRST sources are 10^3 times less common.[11] Furthermore, J1419+3940 is coincident with a star-forming region within the galaxy, which is independent confirmation of association under any source model that scales with star formation. Therefore, from here forward we assume that J1419+3940 is associated with SDSS J141918.81+394035.8. However, if this is not the case and if J1419+3940 is instead a background extragalactic source, we note that the energetic requirements on the transient would further increase.

The association of J1419+3940 with the host allows us to measure a peak spectral luminosity of $2 \times 10^{29} \text{ erg s}^{-1} \text{ Hz}^{-1}$ at 1.4 GHz and $\nu L_\nu \gtrsim 3 \times 10^{38} \text{ erg s}^{-1}$. We do not detect a rising part of the radio light curve, so this is a lower limit on the peak luminosity.

3.3. Search for High-energy Counterparts

We have examined the 4Br BATSE GRB catalog (Paciesas et al. 1999) and NASAs "GRBCAT" compilation[12] for possible GRBs coincident with J1419+3940 and occurring prior to our earliest radio detection of J1419+3940 in November 1993. We find one burst, GRB 921220, whose error circle encompasses our position for J1419+3940. However, the positional uncertainty for this burst is enormous, covering more than 1500 deg^2 ($\sim$4% of the entire sky), and we thus do not find this coincidence

---

[10] The *WISE* emission from SDSS J141918.81+394035.8 plus the FIRST detection of J1419+3940 gave the galaxy an apparent radio to infrared flux ratio otherwise seen only for radio-loud active galactic nuclei at redshifts $z > 2$ (Collier et al. 2014).

[11] In fact, J1419+3940 is among the most variable FIRST sources known (Gal-Yam et al. 2006; Thyagarajan et al. 2011).

[12] This also includes GRBs detected by other missions and by the interplanetary network (IPN); see https://heasarc.gsfc.nasa.gov/grbcat/.

---

significant. The nearest other burst to J1419+3940 was GRB 911024, whose nominal position was $5°.0$ from J1419+3940, and for which the statistical positional uncertainty is a circle of radius $4°.13$. The full positional uncertainty also includes a systematic term (see Briggs et al. 1999), which may make the position of J1419+3940 marginally consistent with GRB 911024. However, given that there are $\sim$1000 known GRBs occurring prior to 1993 November, the chances of any random position on the sky falling within a few degrees of an unrelated GRB is close to unity. We therefore cannot identify any convincing candidates for a GRB associated with J1419+3940.

The lack of any obvious gamma-ray counterpart by BATSE and the IPN is very constraining for nearby GRBs (Cenko et al. 2013). From 1991 to 1993, *Ulysses* was part of the IPN and it had an largely unrestricted view of the sky. *Ulysses* was essentially flux complete to BATSE GRBs above $10^{-4} \text{ erg cm}^{-2}$ (Briggs et al. 1999; Hurley et al. 1999). Most GRBs have an isotropic energy greater than 10^{51} erg in gamma-rays (Amati et al. 2002; Zhang et al. 2009), which corresponds to a fluence of $10^{-3} \text{ erg cm}^{-2}$ at a distance of 87 Mpc. The nondetection by both BATSE and the IPN effectively rules out the presence of an on-axis GRB. It would not, however, necessarily rule out the presence of less-energetic ("low-luminosity") GRBs, which have isotropic energies $\sim 10^{48}$–10^{50} erg (e.g., Kaneko et al. 2007) and have been argued on theoretical grounds to originate from a distinct emission mechanism, such as shock break-out, that is more isotropic than the jetted GRB emission (e.g., Nakar & Sari 2012).

We searched for archival X-ray data at the location J1419+3940. The only observations we found were taken in the second half of 1990, by the *ROSAT* Position Sensitive Proportional Counter (PSPC) as part of the *ROSAT* all-sky survey. There is no apparent source at the position of J1419+3940 in an effective exposure time of 1200 s, from which we estimate an upper limit on the background-corrected count rate of 8.3×10^{-3} counts sec^{-1}. Using the Galactic H I column in this direction of $8.7 \times 10^{19} \text{ cm}^{-2}$ (Kalberla et al. 2005) and assuming a power-law spectrum with a photon index $\Gamma = 2$, the corresponding limit on the unabsorbed flux (0.1–2.4 keV) is $8.6 \times 10^{-14} \text{ erg cm}^{-2} \text{ s}^{-1}$.

We also obtained new X-ray observations of J1419+3940, using the X-Ray Telescope (XRT) on board the *Neil Gehrels Swift Observatory*. The observations took place on 2018 September 16, with an exposure time of 2030 s. No counts were detected at or near the position of J1419+3940, with an upper limit on the background-corrected count rate of 1.5×10^{-3} counts sec^{-1}. Making the same assumptions as above for *ROSAT*, the implied limit on the unabsorbed flux (0.2–10 keV) is $4.7 \times 10^{-14} \text{ erg cm}^{-2} \text{ s}^{-1}$, or about twice as deep as the *ROSAT* observations when compared over consistent energy ranges.

3.4. Rates

J1419+3940 is the only non-nuclear FIRST source found to be so strongly variable (Table 1) in comparison to VLASS, and here we estimate the volumetric rate of J1419+3940-like transients. While the study of Ofek (2017) is complete above 1.5 mJy, we estimate that J1419+3940 would only have been identified if it were brighter than roughly 4 mJy at peak, as this would require an unphysically steep spectral index when compared between 1.4 and 3 GHz. From Figure 1, we see that the source exceeded 4 mJy for a window of $\Delta t \sim 2000$ days.

The radio catalog was drawn from the FIRST survey, which covered $\Delta\Omega \sim 10{,}600$ deg^2 or 25% of the sky. VLASS epoch 1.1 covers half of the visible sky and about half of the Ofek (2017) catalog, so we estimate its completeness relative to FIRST as $f_{\rm VLASS} \sim 0.5$. Ofek (2017) estimated the completeness of his spectroscopic galaxy sample as roughly $f_{\rm spec} \sim 30\%$ of the stellar luminosity out to distance of $d \sim 108$ Mpc. If we assume that the event rate scales with stellar luminosity, we find a volumetric rate of

$$\mathcal{R} \approx \frac{1\ \text{event}}{\Delta t\,(f_{\rm spec} f_{\rm VLASS}\,\Delta\Omega d^3/3)} \approx 900\ \text{Gpc}^{-3}\ \text{yr}^{-1}. \qquad (1)$$

This rate is only accurate to an order of magnitude due to uncertainties in estimating its timescale, galaxy selection, and human bias. We conservatively define the rate constraint as a 95% confidence interval on a Poisson rate of 50–4200 Gpc^{-3} yr^{-1} (Gehrels 1986).

For comparison, the rate of on-axis long GRBs (LGRBs) with $E_{\rm K} \gtrsim 10^{51}$ erg is $\mathcal{R}_{\rm LGRB}(z=0) \approx 0.3$ Gpc^{-1} yr^{-1} (Guetta et al. 2005). For a beaming-correction of $f_{\rm b}^{-1} = 200$ (Goldstein et al. 2016), we expect a true off-axis LGRB rate of $\mathcal{R}_{\rm off\text{-}axis\ LGRB} \approx 60$ Gpc^{-3} yr^{-1}. This rate is consistent with the estimated rate for J1419+3940-like transients.

3.5. Summary

J1419+3940 is a radio transient characterized by

1. a peak transient luminosity at 1.4 GHz of 2×10^{29} erg s^{-1} Hz^{-1} or $\nu L_\nu \gtrsim 3 \times 10^{38}$ erg s^{-1},
2. a half-peak decay time of $\sim$3 years at 1.4 GHz with detections spanning 21.5 years,
3. a radio spectral index ($S_\nu \propto \nu^\alpha$) that evolves from $> +0.6$ at peak to ~ -0.6 at late times,
4. an association with a star-forming region in a dwarf galaxy,
5. no associated GRB, and
6. an inferred rate between 50 and 4200 Gpc^{-3} yr^{-1} (95% confidence interval).

The location of the transient at the edge of its host argues that it is not associated with some exceptional flare or mode change in an active galactic nucleus. Extreme scattering events and other radio propagation-related phenomena have not been observed to magnify to the degree seen for J1419+3940 (Bannister et al. 2016), so we conclude that it is likely an energetic transient.

The peak detected radio luminosity of J1419+3940 exceeds that of supernovae associated with low circumburst densities, such as SN Ia ($< 10^{25}$ erg s^{-1} Hz^{-1}; Chomiuk et al. 2012) and short GRBs ($< 10^{29}$ erg s^{-1} Hz^{-1} on timescales of years; Metzger & Bower 2014; Fong et al. 2016). The long timescale of J1419+3940 is similar to that observed for supernovae in dense environments (e.g., SN IIp and IIn; Weiler et al. 1991; Chandra et al. 2015), but systems with similar rise times to J1419+3940 are much less luminous. Figure 3 compares J1419+3940 with radio supernovae in which the emission is produced by the shock interaction between the supernova ejecta and a dense wind surrounding the progenitor star (e.g., Weiler et al. 2002). As J1419+3940 was only observed to fade, we use its half-peak decay time as an upper limit its rise time. J1419+3940 is at least an order of magnitude more luminous at 1.4 GHz than known radio supernovae. As discussed in
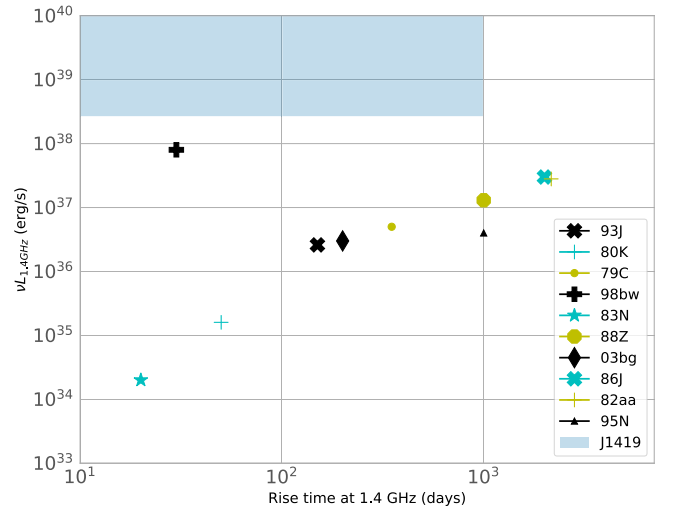
Figure 3. Radio luminosity versus rise time at 1.4 GHz for a sample of radio supernovae with emission produced by shock interaction. J1419+3940 is only seen as a fading radio transient, so the allowed region in blue is defined by a lower limit on peak luminosity and upper limit on its rise time (assuming that it rises faster than it fades). SN 1982aa (a.k.a. Mrk 297A; Yin 1994) was very luminous, but best characterized at 5 GHz. We scale the luminosity and time to peak by the standard model for radio emission from shock-interaction supernovae (Chevalier 1982).

Section 4.1.1, a radio supernova with an unprecedented high luminosity powered by shock interaction would evolve significantly slower than J1419+3940. Furthermore, Type IIn supernovae are observed in a range of (generally massive) host galaxies and thus, as in the case of neutron star mergers, the very low-mass host of J1419 would be unexpected (e.g., van Dyk et al. 1996).

Figure 3 shows that the most similar radio supernova to J1419+3940 is SN 1998bw, the first supernova associated with a GRB (Kulkarni et al. 1998; Weiler et al. 2001). The limits on radio timescale and luminosity of J1419+3940 are consistent with observations of long GRBs (Chandra & Frail 2012) and TDEs (Berger et al. 2012; Alexander et al. 2016) and with theoretical predictions for the class of transients powered by magnetar spin-down (e.g., Metzger et al. 2015a, 2017; Murase et al. 2016; Margalit et al. 2018). The host galaxy is similar to those known to host long GRBs and superluminous supernovae (Fruchter et al. 2006; Lunnan et al. 2015).

Finally, we note that there may be a radio transient with measured luminosity that is a potential analog to J1419+3940. J060938−333508 was a transient detected in a single epoch of an 843 MHz survey of the southern sky (Bannister et al. 2011). It was seen in projection on the disk (non-nuclear) of a galaxy at $z = 0.037$, implying a luminosity 6×10^{29} erg cm^{-2} s^{-1} with an unconstrained timescale. No optical or high-energy transient has been associated with this event.

4. Transient Origin

In this section we consider possible origins of J1419+3940. We begin with most commonly considered type of extragalactic radio transients, namely that created as the high-velocity ejecta from an explosive event, such as a GRB, interacts with its gaseous external environment. Then, we explore an alternative hypothesis that J1419+3940 is the young wind nebula of a compact object, such as a flaring magnetar, embedded within a slower-expanding supernova ejecta shell.

4.1. Synchrotron Blast Waves

4.1.1. General Considerations

Metzger et al. (2015b) derived general constraints on the light curves of synchrotron radio transients from explosions interacting with a gaseous external medium. They consider the ejection of material with a kinetic energy of $E_K = 10^{51} E_{K,51}$ erg and an initial velocity of $v_i = \beta_i c$ (corresponding to an initial Lorentz factor of $\Gamma_i = [1 - \beta_i^2]^{-1/2}$) into an ambient medium of constant density $n = 1 n_0$ cm^{-3}. The ejecta transfer their energy to the ambient medium on a deceleration timescale

$$t_{\rm dec} \approx R_{\rm dec}\big/2c\beta_i\Gamma_i^2 \approx 115 \text{ days } E_{K,51}^{1/3} n_0^{-1/3} \beta_i^{-5/3} \Gamma_i^{-8/3}. \quad (2)$$

where $R_{\rm dec}$ is the characteristic radius at which the ejecta have swept up a mass $\sim 1/\Gamma_i$ of their own mass. The timescale $t_{\rm dec}$ defines a lower limit on the rise time to peak for radio transients (see below).

If the observing frequency ($\nu_{\rm obs} = 1.4\,\nu_{1.4}$ GHz) is located above both the synchrotron peak frequency (ν_m) and the self-absorption frequency (ν_a), then the peak brightness is achieved at $t_{\rm dec}$, and is given by (Nakar & Piran 2011),

$$F_{\nu,\rm dec} \approx 70 \text{ mJy } E_{K,51}^{4/5} n_0^{4/5} \epsilon_{e,-1}^{6/5} \epsilon_{B,-2}^{4/5} \beta_i^{9/4} \nu_{1.4}^{-0.6}, \quad (3)$$

where we have scaled the distance to that of J1419+3940. We make the standard assumption that electrons are accelerated at the shock front into a power-law distribution in momentum with slope p (as predicted by the theory of Fermi acceleration at shocks; Blandford & Eichler 1987) and that $\epsilon_B = 0.01\,\epsilon_{B,-2}$ and $\epsilon_e = 0.1\,\epsilon_{e,-1}$ are the fractions of post-shock energy in the magnetic field and relativistic electrons, respectively. We have taken $p = 2.2$ for consistency with the late-time 1.4/3 GHz spectral index of J1419+3940, assuming that it arises from optically thin synchrotron emission with $F_\nu \propto \nu^{-(p-1)/2}$. The rise time can be longer than $t_{\rm obs}$, and the peak flux somewhat lower, at observing frequencies below the self-absorption frequency

$$\nu_{\rm sa}(t_{\rm dec}) \approx 0.75 \text{ GHz } E_{K,51}^{0.11} n_0^{0.55} \epsilon_{e,-1}^{0.39} \epsilon_{B,-2}^{0.34} \beta_i^{1.23}. \quad (4)$$

Relativistic transients, such as GRBs and jetted TDEs, produce ultra-relativistic ejecta in tightly collimated jets. Less-relativistic transients produce essentially spherical ejecta with isotropic emission at all times. However, relativistic transients viewed in an initial off-axis direction can also be approximated as being spherically symmetric once the shocked matter decelerates to sub-relativistic velocities and spreads laterally into the observer's line of sight (e.g., Zhang & MacFadyen 2009; Wygoda et al. 2011). At this point the radio emission is no longer strongly beamed, and $t_{\rm dec}$ and $F_{\nu,\rm dec}$ can be approximated using a mildly relativistic value $\beta_i \approx 0.5$.

We focus our analysis of J1419+3940 in the case of non-relativistic ejecta, or an initially relativistic but off-axis jet. At the relatively low observing frequencies of interest, an off-axis viewing angle is the most likely configuration for a volume- or flux-limited sample of radio transients (Metzger et al. 2015b). From Equation (3), we then see that for the fiducial values of the microphysical parameters and an external density $n_0 \sim 1$–10 cm^{-1} typical of the average ISM of a star-forming galaxy or the circumburst environment of a massive star, explaining the peak 1.4 GHz flux $\gtrsim 20$ mJy for J1419+3940

requires an initially relativistic explosion ($\beta_i \approx 0.5$) with a kinetic energy $E_K \sim 3 \times 10^{50}$–$3 \times 10^{51}$ erg. We can also place an absolute lower limit of $E_K \sim 10^{49}$ erg for the case of equipartition ($\epsilon_e = \epsilon_B \sim 0.5$). For such parameters, the predicted rise time for an off-axis event is $t_{\rm dec} \sim 0.1$–1 years (Equation (2)). The predicted self-absorption frequency $\nu_{\rm sa}(t_{\rm dec}) \gtrsim 0.3$–$3$ GHz (Equation (4)), below which one predicts a spectral turnover to $F_\nu \propto \nu^2$, is also consistent with the early-time nondetection of J1419+3940 at $\nu \leqslant 350$ MHz. The fact that the self-absorption frequency is close to the 1.4 GHz band at the discovery epoch around 1994 also suggests that the transient was detected close to its peak; although a nice consistency check, this makes the earlier archival upper limits (e.g., <25 mJy at 4.85 GHz in 1987) relatively unconstraining.

Alternatively, the peak flux could be consistent with a spherical non-relativistic explosion $\beta_i \ll 1$ with a larger energy $E_K \sim 4 \times 10^{51}$ erg $n_0^{-4/5}(\beta_i/0.3)^{-9/4}$. An example of such a transient is the ejecta from a neutron star merger ($\beta_i \sim 0.1$–0.3), possibly energized by a long-lived magnetar remnant (Metzger & Bower 2014). The rate of neutron star mergers of 1540_{-1220}^{+3200} Gpc^{-3} yr^{-1} inferred from the discovery of GW170817 (Abbott et al. 2017) agrees with that of J1419+3940 (see Section 3.4). However, one reason to disfavor this scenario as compared to the long GRB case is the small size of the star-forming host of J1419+3940; the lowest measured host galaxy mass of a short GRB is $10^{8.8} M_\odot$ (Leibler & Berger 2010), an order of magnitude larger than the host of J1419+3940.

4.1.2. GRB Afterglow

Based on arguments given above, the peak flux and characteristic timescale of J1419+3940 are broadly consistent with arising from a blast wave of energy and external density similar to those that characterize long-duration GRB jets. The long GRB scenario also agrees with the otherwise peculiar host galaxy properties of J1419+3940 and, albeit marginally, estimates of the occurrence rate for off-axis events (Section 3.4).

To explore this connection in greater depth, Figure 4 compares the multi-band light curves of J1419+3940 to theoretical predictions for GRB afterglows based on relativistic hydrodynamical simulations of a relativistic jet interacting with a constant density ISM from the afterglow library models of van Eerten et al. (2012), modified as described by Sironi & Giannios (2013; see below). We explored a range of parameters and tested for consistency with the peak luminosity, timescale of evolution, early-time spectral index, and late-time decay. We find reasonable agreement between radio measurements at 0.35, 1.4, and 3.0 GHz and models for assumed microphysical parameters $\epsilon_e = 0.1$, $\epsilon_B = 0.025$, electron spectral index $p = 2.2$, external density $n = 10$ cm^{-3}, and isotropic jet energy $E_{\rm iso} = 2 \times 10^{53}$ erg, the latter corresponding to a beaming-corrected jet energy of $E_K \approx 10^{51}$ erg. All of these parameters are well within the range of those inferred by modeling the afterglows of on-axis cosmological long GRBs (e.g., Ryan et al. 2015). The implied time of the burst from these models ranges from a few months to a year prior to the first VLA epoch in late 1993.

The observer viewing angle relative to the jet axis, $\theta_{\rm obs}$, is not well constrained by the data, as its value is somewhat degenerate with the assumed microphysical parameters; our "best-fit" model shown in the top panel of Figure 4 has $\theta_{\rm obs} \approx 0.6$, but, as shown in the bottom panel, a range of other
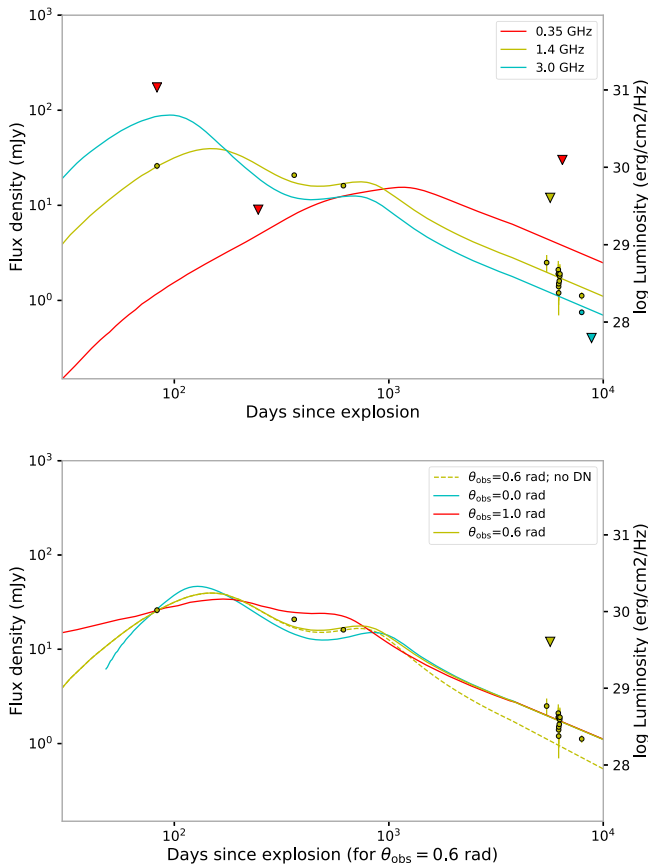
Figure 4. Radio light curve of J1419+3940 starting in 1993 compared to GRB afterglow models that include deep Newtonian corrections (van Eerten et al. 2012; Sironi & Giannios 2013). Top panel: the measurements are shown with red, yellow, and cyan representing 0.35, 1.4, and 3.0 GHz fluxes, respectively. The lines use the same color scheme and show the model fluxes for a GRB viewing angle $\theta_{obs} = 0.6$ rad with explosion date 83 days before the first measurement in late 1993. The isotropic energy is $E_{iso} \approx 2 \times 10^{53}$ erg (giving a beaming-corrected energy of $E_K \sim 10^{51}$ erg), constant ISM density $n = 10$ cm^{-3}, electron index $p = 2.2$, and microphysical parameters $\epsilon_e = 0.1$, $\epsilon_B = 0.025$. Bottom panel: a set of afterglow models is compared to measurements at 1.4 GHz. The $\theta_{obs} = 0.6$ rad model is the same as in the top panel and defines the x-axis labels. The dashed line shows 1.4 GHz predictions without corrections for the deep Newtonian phase. The cyan and red lines show how the 1.4 GHz predictions change for viewing angles of 0.0 (on axis) and 1.0 rad, respectively. The explosion dates are set to fit to the first 1.4 GHz measurement and occur 45 and 180 days before that measurement, respectively.

values $\theta_{obs} \lesssim 1.0$ can also work given the uncertainties. The stronger evidence for an off-axis viewing angle comes from the lack of a coincident GRB (Section 3.3), and from the overall much higher geometrical probability of seeing an off-axis event $\propto 1 - \cos\theta_{obs}$.

We also compared predictions for X-ray flux for the best afterglow models to the measured flux limit in late 1990. For viewing angles $\theta_{obs} \lesssim 0.6$, the models predict a flux above the measured flux limit and lasting for tens of days. The radio data are most consistent with an explosion two to three years later, so the *ROSAT* nondetection is consistent with the off-axis GRB model.

One exception to the generally good afterglow fits is the most recent 3 GHz nondetection by VLASS, which requires a ~50% drop in flux over a baseline of just two years from the prior detection. Such a rapid change is challenging to explain in afterglow models; even large discontinuities in the ISM density

produce at most order-unity changes in flux (Mimica & Giannios 2011), but only over timescales comparable to the source age, which in this case is $\gtrsim 23$ years. Alternatively, this flux drop may be a sign of scintillation-induced fluctuation. Reanalysis of VLASS data or new observations are needed to confirm the flux drop.

If J1419+3940 is indeed a GRB afterglow, its nearby distance and long observational baseline as compared to cosmological GRBs enables an unprecedented test of the late-time behavior of afterglow light curves. The standard prediction for late-time decay is (Frail et al. 2000, 2004)

$$F_\nu \propto t^{-3(5p-7)/10} \underset{p=2.2}{\approx} t^{-1.2} \tag{5}$$

where we have again used $p = 2.2$ for consistency with the late-time 1.4/3 GHz spectral index. However, these models do not generally include the late-time *flattening* of the radio light curve, which is expected as the blast wave enters the so-called "deep Newtonian" regime (Sironi & Giannios 2013). In the deep Newtonian regime, which happens after a timescale $t_{DN} \approx 2.1$ years $E_{K,51}^{1/3} n_0^{-1/3} \epsilon_{e,-1}^{5/6}$, the bulk of the shock-accelerated electrons turn non-relativistic and the theory of Fermi acceleration at shocks (Blandford & Eichler 1987) predicts that the electron spectrum should be a power-law distribution in *momentum* rather than energy. In that case, the light curve is predicted to decay as a shallower power law given by

$$F_\nu \propto t^{-3(p+1)/10} \underset{p=2.2}{\approx} t^{-0.96}, \tag{6}$$

where p is the electron distribution power-law slope.

The bottom panel of Figure 4 shows that, if we were to neglect the physically motivated deep Newtonian correction, our model would underpredict the late-time 1.4 GHz flux measurements by nearly a factor of 2. Our observations of J1419+3940 may thus provide some of the first evidence that GRB afterglows decay at late times in a way that is consistent with predictions for the deep Newtonian regime (Sironi & Giannios 2013).

4.2. Magnetar Birth Nebula

Our discussion thus far has focused on radio transients from an external blast wave interacting with surrounding gas. Alternatively, J1419+3940 could be fading emission from the wind nebula powered by a young compact object, such as a flaring magnetar, embedded behind the ejecta of a decades-old supernova remnant (Metzger et al. 2014, 2017; Murase et al. 2016; Margalit et al. 2018; Omand et al. 2018). While these transients are luminous, their long evolution timescale has made it hard to constrain this population. Indeed, such a model was proposed in the context of the quiescent radio source discovered to be spatially coincident with the repeating fast radio burst FRB 121102 (Chatterjee et al. 2017; Metzger et al. 2017), although that source has not been observed long enough to know if it is fading like J1419+3940. The search for these kinds of sources was the original motivation of Ofek (2017) that discovered J1419+3940 with a peak luminosity nearly equal to that of the FRB 121102 quiescent radio source.

In this model, the 1.4 GHz radio emission is obscured by free–free absorption through the supernova ejecta shell for the first couple of decades of its evolution (e.g., Connor et al. 2016; Piro 2016; Margalit et al. 2018), so its explosion would be significantly earlier than implied in the GRB afterglow model.

The nondetection at lower frequencies $\nu \leqslant 350$ Hz around the time of the 1.4 GHz peak flux (just after the ejecta shell has become transparent at this frequency) is also consistent with the ν^{-2} dependence of the free–free opacity. This model would in principle also predict X-ray emission (e.g., due to higher-energy electron/positron pairs injected by the magnetar's rotational energy). However, the predicted X-ray luminosity is more theoretically uncertain than the radio emission (e.g., because it depends on the magnetic field strength and pair multiplicity of the magnetar wind) and therefore it is difficult to compare to the *ROSAT*/*Swift* upper limits.

The evolution and spectrum of the radio light curve in this model is uncertain, as it depends on poorly understood details of the rate at which magnetic fields and electrons are injected into the nebula (e.g., Margalit et al. 2018). Nevertheless, the present-day power-law spectrum of J1419+3940 between 1.4 and 3 GHz is consistent with that measured at low frequencies for the quiescent source of FRB 121102 (Chatterjee et al. 2017). If the majority of FRBs share the same luminosity function as FRB 121102, the formation rate of FRB-producing objects is also consistent, albeit with large uncertainties, with that of long-duration GRBs and superluminous supernovae[13] for an assumed burster lifetime of decades to centuries (Lu & Kumar 2016; Law et al. 2017; Nicholl et al. 2017b). Based on rate considerations, J1419+3940 therefore also seems consistent with this model. This model predicts that J1419+3940 is a source of FRB emission and would be detectable if beamed in our direction. Future monitoring of this source is strongly encouraged.

5. Conclusions

We have discovered a decades-long, luminous radio transient, FIRST J141918.9+394036, likely hosted by the dwarf galaxy SDSS J141918.81+394035.8 at a redshift $z = 0.01957$. The energy, timescale, host galaxy, and other properties of J1419+3940 suggest that this source is most likely an off-axis long-duration GRB. If so, the slow ($\sim t^{-1}$) decay of the radio afterglow confirms predictions for shock physics at late times (Sironi & Giannios 2013). The energetics of the transient are also consistent with the ejecta from a binary neutron star merger, though the association with a star-forming region in a small host galaxy would be in tension with associations of short duration GRBs, which are typically older stellar populations and $\sim$100 times more massive. We also discuss the more speculative possibility that J1419+3940 is a wind nebula produced in the aftermath of a magnetar-powered supernova. While the energy output of a newborn magnetar is poorly constrained by previous observations, such a scenario is also consistent with the luminosity, duration, and radio flux decay for J1419+3940. Confirming the presence of a young magnetar in J1419+3940 would support arguments that FRBs are born as luminous radio transients (Margalit & Metzger 2018).

The detection of the radio afterglow of an orphan GRB would be the first of its kind (see also Cenko et al. 2013, 2015) and improves the prospects for the radio discovery of extragalactic transients. We note that J1419+3940 was not identified as a transient or variable in comparisons of the FIRST and NVSS radio sky surveys (Levinson et al. 2002;

Ofek & Frail 2011) because the two surveys happened to observe this slowly evolving source within a few months of each other. This implies that published limits on radio transient event rates may be weaker than claimed for decades-long transients like J1419+3940.

Furthermore, the brightness and proximity of J1419+3940 implies that it has a relatively high volumetric rate, potentially in tension with predictions for orphan-GRB afterglows. We estimate that J1419+3940 could have been detected if its peak brightness was as low as 4 mJy, equivalent to a 2.5× larger distance. This implies that there may be an order of magnitude more such "anti-transients" to be found as FIRST sources that disappear in the VLASS and a comparable number of transients turning on in new observations. The chance of discovery will be improved with larger spectroscopic galaxy samples, better identification of non-nuclear radio sources, and the integration of archival radio surveys with the search process. New searches for J1419+3940-like radio transients will improve the rate estimate and may reveal that it is inconsistent with that of orphan GRBs.

Independent of the progenitor model, J1419+3940 is the oldest and best-localized luminous radio transient. That makes it a good place to search for remnants, as the ejecta should be transparent to free–free radiation. An FRB search may find bursts regardless of whether or not it is an GRB afterglow or magnetar wind nebula. Milliarcsecond-resolution imaging could distinguish GRBs from magnetar models by measuring the size of the late-time radio emission. New measurements of the late-time radio flux of J1419+3940 are needed to better measure its late-time radio decay and to properly search for scintillation. The presence of refractive scintillation at GHz frequencies is sensitive to spatial structure on a size scale of 10 to 100 μas and would help distinguish between the afterglow and magnetar wind nebula models.

---

[13] Superluminous supernovae have a rate of $\approx$30 Gpc^{-3} yr^{-1} in the local universe (Prajs et al. 2017).

ORCID iDs

C. J. Law ⓘ https://orcid.org/0000-0002-4119-9963
B. M. Gaensler ⓘ https://orcid.org/0000-0002-3382-9558
B. D. Metzger ⓘ https://orcid.org/0000-0002-4670-7509
E. O. Ofek ⓘ https://orcid.org/0000-0002-6786-8774

References

Abbott, B. P., Abbott, R., Abbott, T. D., et al. 2017, PhRvL, 119, 161101
Abolfathi, B., Aguado, D. S., Aguilar, G., et al. 2018, ApJS, 235, 42
Alexander, K. D., Berger, E., Guillochon, J., Zauderer, B. A., & Williams, P. K. G. 2016, ApJL, 819, L25
Amati, L., Frontera, F., Tavani, M., et al. 2002, A&A, 390, 81
Appleton, P. N., Fadda, D. T., Marleau, F. R., et al. 2004, ApJS, 154, 147
Bannister, K. W., Murphy, T., Gaensler, B. M., Hunstead, R. W., & Chatterjee, S. 2011, MNRAS, 412, 634
Bannister, K. W., Stevens, J., Tuntsov, A. V., et al. 2016, Sci, 351, 354
Bassa, C. G., Tendulkar, S. P., Adams, E. A. K., et al. 2017, ApJL, 843, L8
Becker, R. H., White, R. L., & Edwards, A. L. 1991, ApJS, 75, 1
Becker, R. H., White, R. L., Gregg, M. D., et al. 2000, ApJ, 538, 72
Becker, R. H., White, R. L., & Helfand, D. J. 1995, ApJ, 450, 559
Bell, M. E., Fender, R. P., Swinbank, J., et al. 2011, MNRAS, 415, 2
Berger, E., Zauderer, A., Pooley, G. G., et al. 2012, ApJ, 748, 36
Blandford, R., & Eichler, D. 1987, PhR, 154, 1
Bower, G. C., Croft, S., Keating, G., et al. 2010, ApJ, 725, 1792
Briggs, M. S., Pendleton, G. N., Kippen, R. M., et al. 1999, ApJS, 122, 503
Cenko, S. B., Kulkarni, S. R., Horesh, A., et al. 2013, ApJ, 769, 130
Cenko, S. B., Urban, A. L., Perley, D. A., et al. 2015, ApJL, 803, L24
Chambers, K. C., Magnier, E. A., Metcalfe, N., et al. 2016, arXiv:1612.05560
Chandra, P., Chevalier, R. A., Chugai, N., Fransson, C., & Soderberg, A. M. 2015, ApJ, 810, 32
Chandra, P., & Frail, D. A. 2012, ApJ, 746, 156
Chang, Y.-Y., van der Wel, A., da Cunha, E., & Rix, H.-W. 2015, ApJS, 219, 8
Chatterjee, S., Law, C. J., Wharton, R. S., et al. 2017, Natur, 541, 58
Chevalier, R. A. 1982, ApJ, 259, 302
Chomiuk, L., Soderberg, A. M., Moe, M., et al. 2012, ApJ, 750, 164
Collier, J. D., Banfield, J. K., Norris, R. P., et al. 2014, MNRAS, 439, 545
Condon, J. J., & Broderick, J. J. 1985, AJ, 90, 2540
Condon, J. J., Cotton, W. D., Greisen, E. W., et al. 1998, AJ, 115, 1693
Connor, L., Sievers, J., & Pen, U.-L. 2016, MNRAS, 458, L19
Croft, S., Bower, G. C., Ackermann, R., et al. 2010, ApJ, 719, 45
Dey, A., Schlegel, D. J., Lang, D., et al. 2018, AJ, submitted (arXiv:1804.08657)
Douglas, J. N., Bash, F. N., Bozyan, F. A., Torrence, G. W., & Wolfe, C. 1996, AJ, 111, 1945

Ficarra, A., Grueff, G., & Tomassetti, G. 1985, A&AS, 59, 255
Fong, W., Metzger, B. D., Berger, E., & Özel, F. 2016, ApJ, 831, 141
Frail, D. A., Kulkarni, S. R., Sari, R., et al. 2001, ApJL, 562, L55
Frail, D. A., Metzger, B. D., Berger, E., Kulkarni, S. R., & Yost, S. A. 2004, ApJ, 600, 828
Frail, D. A., Soderberg, A. M., Kulkarni, S. R., et al. 2005, ApJ, 619, 994
Frail, D. A., Waxman, E., & Kulkarni, S. R. 2000, ApJ, 537, 191
Fruchter, A. S., Levan, A. J., Strolger, L., et al. 2006, Natur, 441, 463
Gal-Yam, A., Ofek, E. O., Poznanski, D., et al. 2006, ApJ, 639, 331
Gehrels, N. 1986, ApJ, 303, 336
Gehrels, N., Chincarini, G., Giommi, P., et al. 2004, ApJ, 611, 1005
Goldstein, A., Connaughton, V., Briggs, M. S., & Burns, E. 2016, ApJ, 818, 18
Gregory, P. C., Scott, W. K., Douglas, K., & Condon, J. J. 1996, ApJS, 103, 427
Guetta, D., Piran, T., & Waxman, E. 2005, ApJ, 619, 412
Hancock, P. J., Murphy, T., Gaensler, B. M., Hopkins, A., & Curran, J. R. 2012, MNRAS, 422, 1812
Hancock, P. J., Trott, C. M., & Hurley-Walker, N. 2018, PASA, 35, e011
Helfand, D. J., White, R. L., & Becker, R. H. 2015, ApJ, 801, 26
Hurley, K., Briggs, M. S., Kippen, R. M., et al. 1999, ApJS, 120, 399
Intema, H. T., Jagannathan, P., Mooley, K. P., & Frail, D. A. 2017, A&A, 598, A78
Japelj, J., Vergani, S. D., Salvaterra, R., Hunt, L. K., & Mannucci, F. 2016, A&A, 593, A115
Kalberla, P. M. W., Burton, W. B., Hartmann, D., et al. 2005, A&A, 440, 775
Kaneko, Y., Ramirez-Ruiz, E., Granot, J., et al. 2007, ApJ, 654, 385
Kaplan, D. L., Cordes, J. M., Condon, J. J., & Djorgovski, S. G. 2000, ApJ, 529, 859
Kasen, D., & Bildsten, L. 2010, ApJ, 717, 245
Kashiyama, K., & Murase, K. 2017, ApJL, 839, L3
Kulkarni, S. R., Frail, D. A., Wieringa, M. H., et al. 1998, Natur, 395, 663
Lane, W. M., Cotton, W. D., van Velzen, S., et al. 2014, MNRAS, 440, 327
Law, C. J., Abruzzo, M. W., Bassa, C. G., et al. 2017, ApJ, 850, 76
Law, N. M., Kulkarni, S. R., Dekany, R. G., et al. 2009, PASP, 121, 1395
Leibler, C. N., & Berger, E. 2010, ApJ, 725, 1202
Levinson, A., Ofek, E. O., Waxman, E., & Gal-Yam, A. 2002, ApJ, 576, 923
Lu, W., & Kumar, P. 2016, MNRAS, 461, L122
Lunnan, R., Chornock, R., Berger, E., et al. 2015, ApJ, 804, 90
Margalit, B., & Metzger, B. D. 2018, ApJL, submitted (arXiv:1808.09969)
Margalit, B., Metzger, B. D., Berger, E., et al. 2018, MNRAS, submitted (arXiv:1806.05690)
Masci, F. J., Laher, R. R., Rebbapragada, U. D., et al. 2017, PASP, 129, 014002
McMullin, J. P., Waters, B., Schiebel, D., Young, W., & Golap, K. 2007, in ASP Conf. Ser. 376, Astronomical Data Analysis Software and Systems XVI, ed. R. A. Shaw, F. Hill, & D. J. Bell (San Francisco, CA: ASP), 127
Metzger, B. D., Berger, E., & Margalit, B. 2017, ApJ, 841, 14
Metzger, B. D., & Bower, G. C. 2014, MNRAS, 437, 1821
Metzger, B. D., Margalit, B., Kasen, D., & Quataert, E. 2015a, MNRAS, 454, 3311
Metzger, B. D., Vurm, I., Hascoët, R., & Beloborodov, A. M. 2014, MNRAS, 437, 703
Metzger, B. D., Williams, P. K. G., & Berger, E. 2015b, ApJ, 806, 224
Mimica, P., & Giannios, D. 2011, MNRAS, 418, 583
Monet, D. G., Levine, S. E., Canzian, B., et al. 2003, AJ, 125, 984
Mooley, K. P., Frail, D. A., Ofek, E. O., et al. 2013, ApJ, 768, 165
Mooley, K. P., Hallinan, G., Bourke, S., et al. 2016, ApJ, 818, 105
Murase, K., Kashiyama, K., & Mészáros, P. 2016, MNRAS, 461, 1498
Murphy, T., Kaplan, D. L., Croft, S., et al. 2017, MNRAS, 466, 1944
Nakar, E., & Piran, T. 2011, Natur, 478, 82
Nakar, E., & Sari, R. 2012, ApJ, 747, 88
Nicholl, M., Guillochon, J., & Berger, E. 2017a, ApJ, 850, 55
Nicholl, M., Williams, P. K. G., Berger, E., et al. 2017b, ApJ, 843, 84
Ochsenbein, F., Bauer, P., & Marcout, J. 2000, A&AS, 143, 23
Ofek, E. O. 2017, ApJ, 846, 44
Ofek, E. O., Breslauer, B., Gal-Yam, A., et al. 2010, ApJ, 711, 517
Ofek, E. O., & Frail, D. A. 2011, ApJ, 737, 45
Ofek, E. O., Frail, D. A., Breslauer, B., et al. 2011, ApJ, 740, 65
Omand, C. M. B., Kashiyama, K., & Murase, K. 2018, MNRAS, 474, 573
Paciesas, W. S., Meegan, C. A., Pendleton, G. N., et al. 1999, ApJS, 122, 465
Piro, A. L. 2016, ApJL, 824, L32
Planck Collaboration, Aghanim, N., Akrami, Y., et al. 2018, arXiv:1807.06209
Prajs, S., Sullivan, M., Smith, M., et al. 2017, MNRAS, 464, 3568
Reines, A. E., Reynolds, M. T., Miller, J. M., et al. 2016, ApJL, 830, L35
Rengelink, R. B., Tang, Y., de Bruyn, A. G., et al. 1997, A&AS, 124, 259
Rowlinson, A., Bell, M. E., Murphy, T., et al. 2016, MNRAS, 458, 3506
Ryan, G., van Eerten, H., MacFadyen, A., & Zhang, B.-B. 2015, ApJ, 799, 3

Sault, R. J., Teuben, P. J., & Wright, M. C. H. 1995, adass IV, 77, 433

Serra, P., Oosterloo, T., Morganti, R., et al. 2012, MNRAS, 422, 1835

Sironi, L., & Giannios, D. 2013, ApJ, 778, 107

The Astropy Collaboration, Price-Whelan, A. M., Sipőcz, B. M., et al. 2018, arXiv:1801.02634

Thyagarajan, N., Helfand, D. J., White, R. L., & Becker, R. H. 2011, ApJ, 742, 49

van Dyk, S. D., Weiler, K. W., Sramek, R. A., et al. 1996, AJ, 111, 1271

van Eerten, H., van der Horst, A., & MacFadyen, A. 2012, ApJ, 749, 44

van Velzen, S., Farrar, G. R., Gezari, S., et al. 2011, ApJ, 741, 73

Weiler, K. W., Panagia, N., & Montes, M. J. 2001, ApJ, 562, 670

Weiler, K. W., Panagia, N., Montes, M. J., & Sramek, R. A. 2002, ARA&A, 40, 387

Weiler, K. W., van Dyk, S. D., Panagia, N., Sramek, R. A., & Discenna, J. L. 1991, ApJ, 380, 161

White, R. L., & Becker, R. H. 1992, ApJS, 79, 331

White, R. L., Becker, R. H., Helfand, D. J., & Gregg, M. D. 1997, ApJ, 475, 479

Woosley, S. E., & Bloom, J. S. 2006, ARA&A, 44, 507

Wygoda, N., Waxman, E., & Frail, D. A. 2011, ApJL, 738, L23

Yin, Q. F. 1994, ApJ, 420, 152

Zauderer, B. A., Berger, E., Soderberg, A. M., et al. 2011, Natur, 476, 425

Zhang, B., Zhang, B.-B., Virgili, F. J., et al. 2009, ApJ, 703, 1696

Zhang, W., & MacFadyen, A. 2009, ApJ, 698, 1261

Zhang, X., Zheng, Y., Chen, H., et al. 1997, A&AS, 121, 59